Progress In Electromagnetics Research M, Vol. 46, 165–172, 2016

Surface-Plasmon-Polaritons at the Interface of Nanostructured Metamaterials

Tatjana Gric*

Abstract—The rigorous modeling and analysis of surface waves at the boundary of two metamaterials are presented. The nature of the phenomenon of the surface-plasmon-polaritons and the influence of various parameters on it are investigated. We have analyzed the properties of structures incorporating nanostructured metamaterials. Surface-plasmon-polaritons at the interface of such metamaterials are studied. We demonstrate the ways to control the properties of the surface waves. Each metamaterial comprises alternating metal and dielectric layers. We analyze the dependence of the dispersion characteristics on the materials employed in metal-dielectric compound. The consistency of the dispersion diagrams and effective permittivity is studied. The Drude model is introduced in the metal dispersion in order to take into account the effects of the structure on dielectric properties.

1. INTRODUCTION

Surface waves open wide avenues for many physical phenomena forming a basis for a number of devices [1–3]. The range of structures capable of supporting surface waves has been expanded due to the invention of metamaterials with controllable electric and magnetic properties [4]. Surface plasmon polaritons (SPPs) are electromagnetic excitations propagating at the interface between a dielectric and a conductor, evanescently confined in the perpendicular direction [5–8]. The properties of confined surface-plasmon-polaritons can be imitated by geometrical induced SPPs, also known as spoof SPPs at lower frequencies being microwaves and terahertz, or even under the limit of a perfect electric conductor. It seems that surface structure may spoof surface plasmons, and the former provides a perfect prototype for structured surfaces [9].

One of the key concepts of the physics of artificial composites (or metamaterials) for electromagnetic waves is the possibility to describe their properties by effective parameters derived under the assumption that the structural elements of such a metamaterial are much smaller than the radiation wavelength.

Anisotropic metamaterials is one outstanding class of metamaterials [10]. It is interesting to notice that its material parameters are not scalars but tensors, with different values of the principle components. Due to this fact, the solutions of the dispersion relations possess elliptic or hyperbolic shapes [11]. The outstanding properties of such anisotropic metamaterials are as follows: negative refraction [12, 13], super-resolution in the far-field through image magnification [14], and enhanced spontaneous emission [15]. It should be mentioned that nanostructured metamaterials presented in this study is the example of anisotropic metamaterials. Periodic metal-dielectric nanostructures open the wide avenues for applications [16–21]. In addition, a lot of investigations have been done in the field of anisotropic metamaterials, both experimentally [22] and theoretically [23–25].

Thus, a huge stream of papers is dedicated to the examination of properties of the metal-dielectric nanostructures [26–28]. However, there is still lack of studies directed towards the investigation of ways to control their properties.

Received 16 December 2015, Accepted 23 February 2016, Scheduled 1 March 2016
* Corresponding author: Tatjana Gric (tatjana.gric@vgtu.lt).
Department of Telecommunication Engineering, Department of Electronic Systems, Vilnius Gedimanas Technical University, Vilnius, Lithuania.

The present paper is devoted to the rigorous modeling and treatment of surface waves at the boundary of two metamaterials that are supposed to be characterized by certain given effective parameters. Firstly, a theoretical model is presented, and then we proceed by mentioning various metamaterial structures where the surface waves can propagate.

2. MODELLING AND THE ANALYTICAL SOLUTION

The system considered in our study is a nanostructured metamaterial formed by metal and dielectric layers of different thicknesses, as shown in Fig. 1.

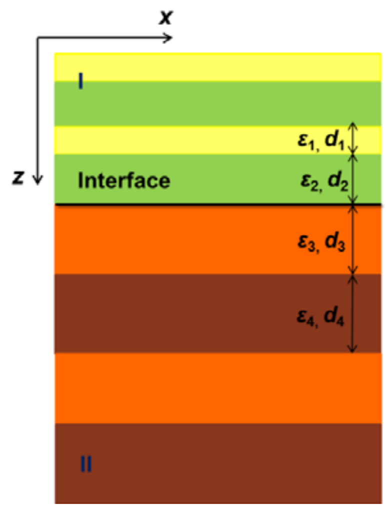

Figure 1. Schematic view of an interface separating two different layered nanostructured metamaterials formed by alternating metal and dielectric layers.

One can apply the effective-medium approach if the wavelength of radiation is much larger than the thickness of any layer. It is based on averaging the structure parameters. As a consequence, it is possible to conclude with the effective homogeneous media for two semi-infinite periodic structures. The effective permittivities are as follows [29]:

$$\varepsilon_{\parallel}^{I} = \frac{\varepsilon_1 d_1 + \varepsilon_2 d_2}{d_1 + d_2} \tag{1a}$$

$$\varepsilon_{\parallel}^{II} = \frac{\varepsilon_3 d_3 + \varepsilon_4 d_4}{d_3 + d_4} \tag{1b}$$

$$\varepsilon_{\perp}^{I} = \frac{\varepsilon_1 \varepsilon_2 \left(d_1 + d_2\right)}{\varepsilon_1 d_2 + \varepsilon_2 d_1}, \tag{2a}$$

$$\varepsilon_{\perp}^{II} = \frac{\varepsilon_3 \varepsilon_4 \left(d_3 + d_4\right)}{\varepsilon_3 d_4 + \varepsilon_4 d_3}, \tag{2b}$$

where subindexes I and II refer to the first and second metamaterial under consideration, respectively. Matching the tangential components of electrical and magnetic fields at the interface implies the dispersion relation for the surface modes localized at the boundary separating two anisotropic media [30]. We assume the permittivities $\varepsilon_{1,3}(\omega)$ to be frequency dependent as the corresponding layers are represented by metals. The mentioned issue is important for both usual plasmon polaritons [31] and surface waves in artificial media [32]. It is interesting to notice that in the case of $\varepsilon_1 = \varepsilon_3$ and $\varepsilon_2 = \varepsilon_4$, the obtained result coincides with the dispersion of a conventional surface plasmon at a metal-dielectric interface and is as follows [30]:

$$\beta = k\sqrt{\frac{\varepsilon_1 \varepsilon_2}{\varepsilon_1 + \varepsilon_2}} \tag{3}$$

In contrary, the dispersion for the case of $\varepsilon_1 = \varepsilon_3$ and $\varepsilon_2 \neq \varepsilon_4$, $d_1 \neq d_2 \neq d_3 \neq d_4$ depends on the thicknesses of the layers employed in the metamaterial as follows:

$$\beta = k\sqrt{\frac{\varepsilon_1^2\varepsilon_2\varepsilon_4\left(d_1+d_2\right)\cdot\left(d_3+d_4\right)\cdot\left(\dfrac{d_1\varepsilon_1+d_2\varepsilon_2}{d_1+d_2}-\dfrac{d_3\varepsilon_1+d_4\varepsilon_4}{d_3+d_4}\right)}{\left(\dfrac{\varepsilon_1\varepsilon_2\left(d_1\varepsilon_1+d_2\varepsilon_2\right)}{d_1\varepsilon_2+d_2\varepsilon_1}-\dfrac{\varepsilon_1\varepsilon_4\left(d_3\varepsilon_1+d_4\varepsilon_4\right)}{d_4\varepsilon_1+d_3\varepsilon_4}\right)\cdot\left(d_1\varepsilon_2+d_2\varepsilon_1\right)\cdot\left(d_4\varepsilon_2+d_3\varepsilon_4\right)}} \tag{4}$$

In case of $\varepsilon_1 \neq \varepsilon_3$ and $\varepsilon_2 \neq \varepsilon_4$, $d_1 = d_2$, $d_3 = d_4$

$$\beta = 2k\sqrt{\left(\varepsilon_1\varepsilon_2\varepsilon_3\varepsilon_4\left(\frac{\varepsilon_1}{2}+\frac{\varepsilon_2}{2}-\frac{\varepsilon_3}{2}-\frac{\varepsilon_4}{2}\right)\right)/\left(\left(\varepsilon_1+\varepsilon_2\right)\cdot\left(\varepsilon_3+\varepsilon_4\right)\cdot\left(\varepsilon_1\varepsilon_2-\varepsilon_3\varepsilon_4\right)\right)} \tag{5}$$

In case of $\varepsilon_1 \neq \varepsilon_3$ and $\varepsilon_2 \neq \varepsilon_4$, $d_1 \neq d_2 \neq d_3 \neq d_4$

$$\beta = k\sqrt{\frac{\varepsilon_1\varepsilon_2\varepsilon_3\varepsilon_4\cdot\left(d_1+d_2\right)\cdot\left(d_3+d_4\right)\cdot\left(\dfrac{d_1\varepsilon_1+d_2\varepsilon_2}{d_1+d_2}-\dfrac{d_3\varepsilon_3+d_4\varepsilon_4}{d_3+d_4}\right)}{\left(\dfrac{\varepsilon_1\varepsilon_2\left(d_1\varepsilon_1+d_2\varepsilon_2\right)}{d_1\varepsilon_2+d_2\varepsilon_1}-\dfrac{\varepsilon_3\varepsilon_4\left(d_3\varepsilon_3+d_4\varepsilon_4\right)}{d_3\varepsilon_4+d_4\varepsilon_3}\right)\cdot\left(d_1\varepsilon_2+d_2\varepsilon_1\right)\cdot\left(d_3\varepsilon_4+d_4\varepsilon_3\right)}} \tag{6}$$

It is of particular importance that the results in Eqs. (3)–(6) are valid only under the condition of surface confinement, which can be presented in the following way [30]:

$$\begin{cases} k_{z,I}^2 = \left(k^2-\beta^2/\varepsilon_{||}^I\right)\varepsilon_\perp^I < 0, \\ k_{z,II}^2 = \left(k^2-\beta^2/\varepsilon_{||}^{II}\right)\varepsilon_\perp^{II} < 0. \end{cases} \tag{7}$$

Assume that we are considering the structures with $\mu = \frac{d_1}{d_2} = \frac{d_4}{d_3}$ and equal periods, i.e., $d_1 + d_2 = d_3 + d_4 = D$. Doing so, the condition of the mode confinement is as follows:

$$\varepsilon_1^2 + \varepsilon_2^2 - |\varepsilon_1|\,|\varepsilon_2|\left(\mu+\frac{1}{\mu}\right) < 0 \tag{8}$$

Equation (8) generates a range of frequencies where the surface mode is confined considering the filling factor μ as a parameter. This range is presented in Fig. 3 as blue area for the case Ag/Al_2O_3-Ag/Al_2O_3. Moreover, the limiting cases should be mentioned. First, this is the case when the filling factor μ vanishes — in this case, we have a conventional surface plasmon resonance at the interface between two isotropic media, and the plasmon is confined for all frequencies. The other case is when the filling factor is unity, i.e., there is no boundary between metal-dielectric structures and thus we are dealing with only one infinite periodic structure. In this case, the surface state can only be confined exactly at the frequency of a bulk plasmon.

3. SIMULATION RESULTS AND DISCUSSIONS

To obtain the insight into the propagation characteristics associated with the surface waves, numerical calculations have been performed using the analytical solutions presented above. This brings about interesting phenomena which is new and important for an actual design.

In this section, several examples of polaritons at the boundary of two metamaterials are given. To illustrate the properties of SPPs we plot the wave vector β (Eqs. (3)–(6)) as a function of the frequency. To exemplificatively demonstrate the properties of surface waves, we adopt a lossless Drude model to characterize the metals (silver or gold) in which the permittivities are expressed as $\varepsilon_{1,3} = 1 - \omega_{p1,3}^2/\omega^2$, where $\omega_{p1,3}$ are the plasma frequencies. It should be mentioned that for silver $\omega_p = 9.5\,\text{eV}$ [33] and for gold $\omega_p = 10\,\text{eV}$ [30].

3.1. Engineered Effective Permittivity of the Nanostructured Hyperbolic Metamaterials

The asymptotic frequencies of the surface waves can be tuned by changing the metamaterial design and its effective properties. The perpendicular effective permittivities of the metamaterials are displayed in Fig. 2 showing how they vary for different structure cases. The peak positions can be controlled through adjusting the structure of the metamaterials under consideration. It should be noted that the resonant behavior of $\varepsilon_\perp$ can be regulated by changing the permittivity of the dielectric employed in the metamaterial (Fig. 2(a)). Moreover, the resonant frequency of $\varepsilon_\perp$ shifts to the higher frequency as the value of the permittivity of the dielectric in the metamaterial is decreasing. Also, it is of particular importance that the frequency of the negative $\varepsilon_\perp$ is also extended simultaneously. These properties are substantial in order to control the surface wave. Particularly, the frequency ranges of surface wave can be tuned by changing the metamaterial design, which is consistent with the dependence of the negative permittivity $\varepsilon_\perp$ on the metamaterial properties as shown in Fig. 2.

Thus, it should be stated that Ag/Al_2O_3 [34] has the smallest resonance frequency (Fig. 2(b)). The resonant frequency of Ag/Al_2O_3 being smaller than of other metal/dielectric compounds leads to the

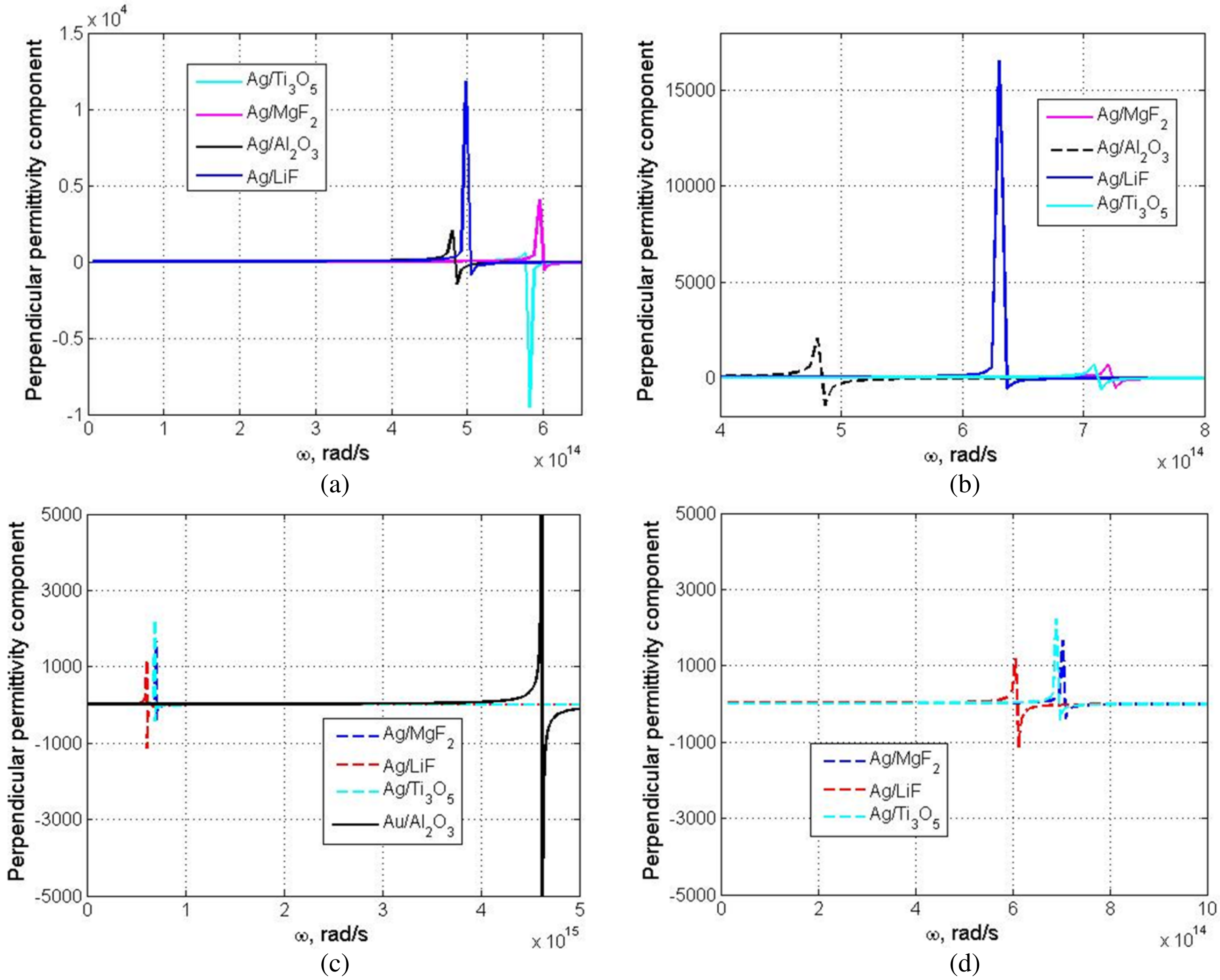

Figure 2. The influence of the material design on the real part of $\varepsilon_\perp$, if (a) $\varepsilon_1 = \varepsilon_3$, $\varepsilon_2 = \varepsilon_4$ and $d_1 \neq d_2 \neq d_3 \neq d_4$; $d_1 = 40\,\mathrm{nm}$; $d_2 = 22.5\,\mathrm{nm}$; $d_3 = 30\,\mathrm{nm}$; $d_4 = 33.5\,\mathrm{nm}$; (b) $\varepsilon_1 = \varepsilon_3$, $\varepsilon_2 \neq \varepsilon_4$ and $d_1 \neq d_2 \neq d_3 \neq d_4$; $d_1 = 40\,\mathrm{nm}$; $d_2 = 22.5\,\mathrm{nm}$; $d_3 = 30\,\mathrm{nm}$; $d_4 = 33.5\,\mathrm{nm}$; (c) $\varepsilon_1 \neq \varepsilon_3$ and $\varepsilon_2 \neq \varepsilon_4$, $d_1 = d_2 = 20\,\mathrm{nm}$, $d_3 = d_4 = 30\,\mathrm{nm}$. (d) An enlarged view of the case (c) at the frequency range (0, 10^{15}) rad/s. Dashed and solid lines refer to the metamaterials with subindexes I and II correspondingly.

decrease of the asymptotic frequencies of the dispersion curves (Fig. 3). It can be observed that the resonant frequency shifts to lower frequencies quickly as the permittivity of the dielectric is increased (Fig. 2(b)).

3.2. Surface Waves at the Boundary of the Nanostructured Hyperbolic Metamaterials

We have ignored metal losses in our analysis. Directing towards a realistic examination, however, the permittivities of the metals $\varepsilon_{1,3}$ are not the real-valued constants, thus leading to a non-vanishing imaginary part of the permittivity $\varepsilon_\perp$ of the metal-dielectric compound. The derived equations for the longitudinal propagation constant (Eqs. (4)–(6)) will now be illustrated by means of the dispersion diagrams of the TM modes supported by the considered structure. In Fig. 3 the dispersion curves for the case $\varepsilon_1 = \varepsilon_3$, $\varepsilon_2 = \varepsilon_4$ and $d_1 \neq d_2 \neq d_3 \neq d_4$ are reported. The dispersion curves of spoof SPPs at the boundary of two metamaterials with $d_1 = 40\,\text{nm}$, $d_2 = 22.5\,\text{nm}$, $d_3 = 30\,\text{nm}$, $d_4 = 33.5\,\text{nm}$ are shown in Fig. 3. It is of particular interest to analyze the effect of the employed dielectric on the dispersion curves of spoof SPPs. For this reason four different dielectrics, i.e., Al_2O_3 [34, 35], LiF [36], MgF_2 [37], Ti_3O_5 [38] are suggested for the study. As seen from Fig. 3, the smallest asymptotic frequency is achieved employing the dielectric with the largest permittivity, i.e., Al_2O_3. Moreover, we have employed a Drude-like dielectric function of the following form $\varepsilon_{1,3} = 1 - \omega_{p1,3}^2/(\omega^2 + i\delta\omega)$ with $\delta = 0.0987\,\text{eV}$ [33] to discover the impact of losses to the dispersion curves (presented with dots in Fig. 3). It should be noticed that losses do not make significant impact on the dispersion curves at the frequency range under the consideration. By this reason, we will ignore metal losses in further analysis.

Turning now to the second case under the study, i.e., $\varepsilon_1 = \varepsilon_3$ and $\varepsilon_2 \neq \varepsilon_4$, $d_1 \neq d_2 \neq d_3 \neq d_4$, in Fig. 4, six modes are represented at the boundary of two different metamaterials. As seen from Fig. 4, the smallest asymptotic frequency corresponds to the case Ag/Al_2O_3-Ag/LiF. It is worth mentioning that for cases such as Ag/Al_2O_3-Ag/LiF, Ag/LiF-Ag/Ti_3O_5, Ag/Al_2O_3-Ag/MgF_2, the frequency of the SPPs grows more slowly with increasing β, than dealing with other cases. Moreover, the splitting factor of all the curves, except Ag/Al_2O_3-Ag/LiF, decreases at higher frequencies. The splitting factor here is assumed as the difference in frequency for the chosen propagation constant value.

As in previous cases, the case denoted as $\varepsilon_1 \neq \varepsilon_3$ and $\varepsilon_2 \neq \varepsilon_4$, $d_1 = d_2$, $d_3 = d_4$ will be illustrated by means of the dispersion diagrams of the TM modes. In Fig. 5, six different modes are presented.

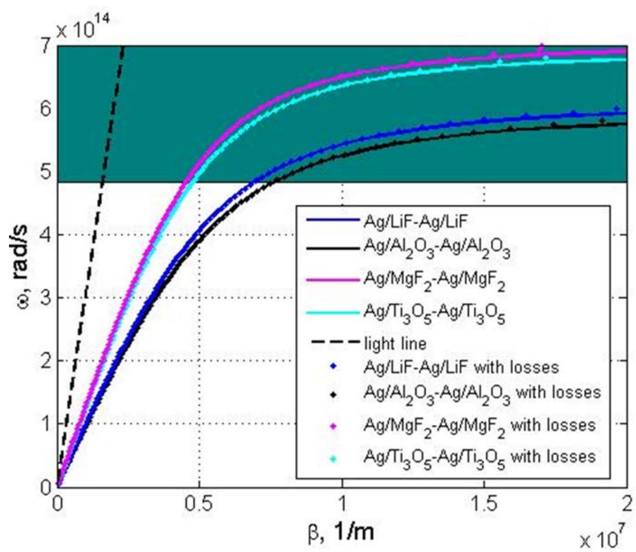

Figure 3. Dispersion curves for spoof SPPs in the case of $\varepsilon_1 = \varepsilon_3$, $\varepsilon_2 = \varepsilon_4$ and $d_1 \neq d_2 \neq d_3 \neq d_4$. Blue area shows the bounds of surface mode existence predicted by effective media approach for the case Ag/Al_2O_3-Ag/Al_2O_3.

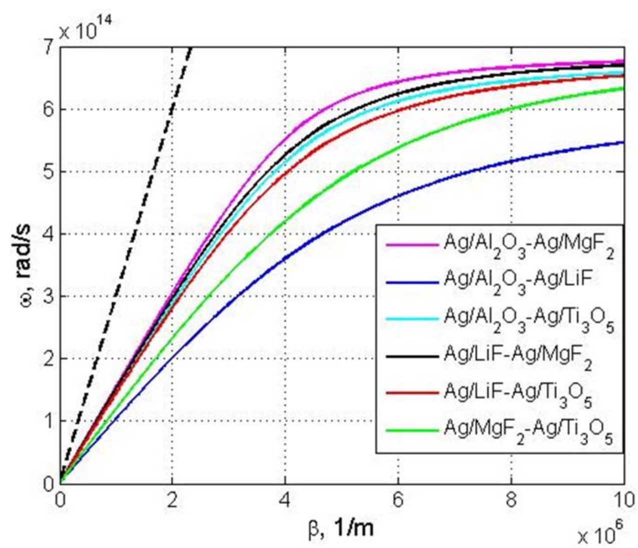

Figure 4. Dispersion curves for spoof SPPs in the case of $\varepsilon_1 = \varepsilon_3$ and $\varepsilon_2 \neq \varepsilon_4$, $d_1 \neq d_2 \neq d_3 \neq d_4$.

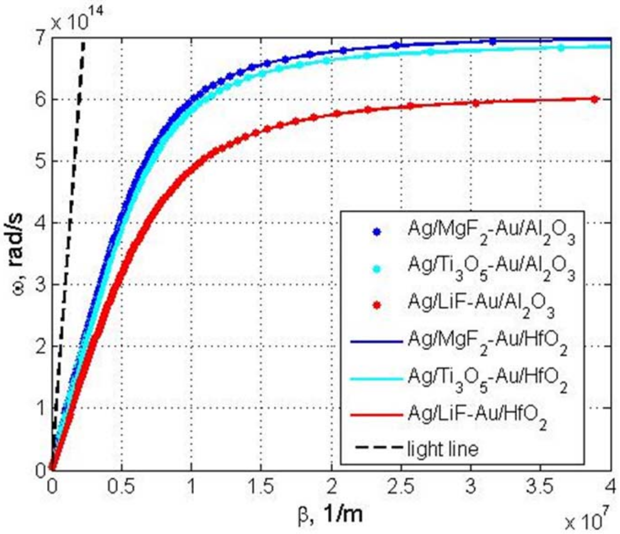

Figure 5. Dispersion curves for spoof SPPs in the case of $\varepsilon_1 \neq \varepsilon_3$ and $\varepsilon_2 \neq \varepsilon_4$, $d_1 = d_2$, $d_3 = d_4$.

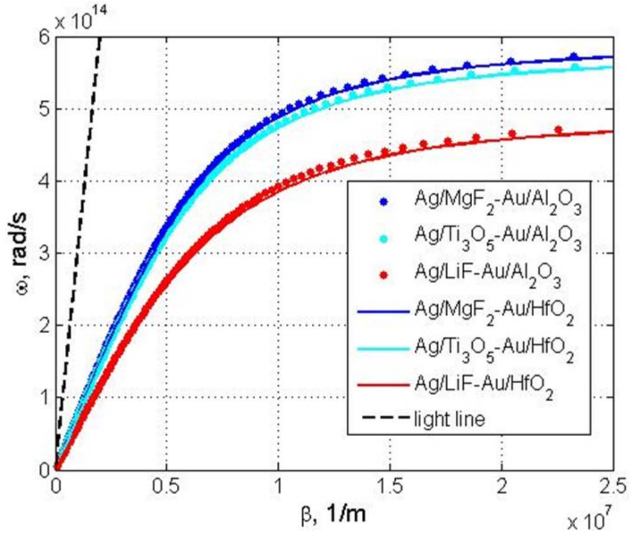

Figure 6. Dispersion curves for spoof SPPs in the case of $\varepsilon_1 \neq \varepsilon_3$ and $\varepsilon_2 \neq \varepsilon_4$, $d_1 \neq d_2 \neq d_3 \neq d_4$.

Actually, we obtain an astonishing result: the dispersion of a (single) interface mode does not depend on the thicknesses of the layers (Eq. (5)).

In Fig. 6, the dispersion curves of six modes are reported in the same frequency range as in Fig. 5 for the case $\varepsilon_1 \neq \varepsilon_3$ and $\varepsilon_2 \neq \varepsilon_4$, $d_1 \neq d_2 \neq d_3 \neq d_4$. All the modes have a similar behavior.

4. CONCLUSION

In conclusion, we have studied surface modes at an interface separating two different layered metal-dielectric structures.

It is found that the perpendicular components of effective permittivity have the resonant behavior, and they can be tuned by changing the metamaterial design. Moreover, the frequency ranges of the surface waves existence are consistent with the resonant frequencies of the perpendicular components. Consequently, the possibilities to tailor the surface waves are suggested. Frequency range of surface wave existence can be engineered by varying metamaterial design.

REFERENCES

1. Yan, H., X. Li, B. Chandra, G. Tulevski, Y. Wu, M. Freitag, W. Zhu, P. Avouris, and F. Xia, "Tunable infrared plasmonic devices using graphene/insulator stacks," *Nat. Nanotechnol.*, Vol. 7, 330, 2012.
2. Viti, L., D. Coquillat, A. Politano, K. A. Kokh, Z. S. Aliev, M. B. Babanly, O. E. Tereshchenko, W. Knap, E. V. Chulkov, and M. S. Vitiello, "Plasma-wave terahertz detection mediated by topological insulators surface states," *Nano Lett.*, Vol. 16, 80, 2016.
3. Politano, A. and G. Chiarello, "Unravelling suitable graphene-metal contacts for graphene-based plasmonic devices," *Nanoscale*, Vol. 5, 8215, 2013.
4. Radkovskaya, A., E. Tatartschuk, O. Sydoruk, E. Shamonina, C. J. Stevens, D. J. Edwards, and L. Solymar, "Surface waves at an interface of two metamaterial structures with interelement coupling," *Phys. Rev. B*, Vol. 82, 045430, 2010.
5. Echtermeyer, T. J., S. Milana, U. Sassi, A. Eiden, M. Wu, E. Lidorikis, and A. C. Ferrari, "Surface plasmon polariton graphene photodetectors," *Nano Lett.*, Vol. 16, 8, 2015.

6. Politano, A. and G. Chiarello, "The influence of electron confinement, quantum size effects, and film morphology on the dispersion and the damping of plasmonic modes in Ag and Au thin films," *Prog. Surf. Sci.*, Vol. 90, 144, 2015.
7. Nechaev, I. A., I. Aguilera, V. De Renzi, A. di Bona, A. Lodi Rizzini, A. M. Mio, G. Nicotra, A. Politano, S. Scalese, Z. S. Aliev, M. B. Babanly, C. Friedrich, S. Blügel, and E. V. Chulkov, "Quasiparticle spectrum and plasmonic excitations in the topological insulator Sb_2Te_3," *Phys. Rev. B*, Vol. 91, 245123, 2015.
8. Politano, A., "Interplay of structural and temperature effects on plasmonic excitations at noble-metal interfaces," *Philos. Mag.*, Vol. 92, 768, 2012.
9. Pendry, J. B., L. Martin-Moreno, and F. J. Garcia-Vidal, "Mimicking surface plasmons with structured surfaces," *Science*, Vol. 305, 847, 2004.
10. Poddubny, A., I. Iorsh, P. Belov, and Y. Kivshar, "Hyperbolic metamaterials," *Nat. Photon.*, Vol. 7, 948, 2013.
11. Jacob, Z., L. V. Alekseyev, and E. Narimanov, "Optical hyperlens: far-field imaging beyond the diffraction limit," *Opt. Express*, Vol. 14, 8247, 2006.
12. Fang, A., T. Koschny, and C. M. Soukoulis, "Optical anisotropic metamaterials: negative refraction and focusing," *Phys. Rev. B*, Vol. 79, 245127, 2009.
13. García-Chocano, V. M., J. Christensen, J. Sa'nchez-Dehesa, "Negative refraction and energy funneling by hyperbolic materials: An experimental demonstration in acoustics," *Phys. Rev. Lett.*, Vol. 112, 144301, 2014.
14. Liu, Z. W., H. Lee, Y. Xiong, C. Sun, and X. Zhang, "Far-field optical hyperlens magnifying sub-diffraction-limited objects," *Science*, Vol. 315, 1686, 2007.
15. Lu, D., J. J. Kan, E. E. Fullerton, and Z. W. Liu, "Enhancing spontaneous emission rates of molecules using nanopatterned multilayer hyperbolic metamaterials," *Nat. Nanotech.*, Vol. 9, 48, 2014.
16. Ramakrishna, S. A. and J. B. Pendry, "Optical gain removes absorption and improves resolution in a near-field lens," *Phys. Rev. B*, Vol. 67, 201101, 2003.
17. Belov, P. A. and Y. Hao, "Subwavelength imaging at optical frequencies using a transmission device formed by a periodic layered metal-dielectric structure operating in the canalization regime," *Phys. Rev. B*, Vol. 73, 113110, 2006.
18. Li, X., S. He, and Y. Jin, "Subwavelength focusing with a multilayered Fabry-Perot structure at optical frequencies," *Phys. Rev. B*, Vol. 75, 045103, 2007.
19. Liu, Z., H. Lee, Y. Xiong, C. Sun, and X. Zhang, "Optical hyperlens magnifying sub-diffraction-limited objects," *Science*, Vol. 315, 1686, 2007.
20. Xiong, Y., Z. Liu, and X. Zhang, "Projecting deep-subwavelength patterns from diffraction-limited masks using metal-dielectric multilayers," *Appl. Phys. Lett.*, Vol. 93, 111116, 2008.
21. Engheta, N., "Circuits with light at nanoscales: Optical nanocircuits inspired by metamaterials," *Science*, Vol. 317, 1698, 2007.
22. Hoffman, A. J., L. Alekseyev, S. S. Howard, K. J. Franz, D. Wasserman, V. A. Podolskiy, E. E. Narimanov, D. L. Sivco, and C. Gmachl, "Negative refraction in semiconductor metamaterials," *Nature Mater.*, Vol. 6, 946, 2007.
23. Smith, D. R. and D. Schurig, "Electromagnetic wave propagation in media with indefinite permittivity and permeability tensors," *Phys. Rev. Lett.*, Vol. 90, 077405, 2003.
24. Scalora, M., G. D'Aguanno, N. Mattiucci, M. J. Bloemer, D. De Ceglia, M. Centini, A. Mandatori, C. Sibilia, N. Akozbek, M. G. Cappeddu, M. Fowler, and J. W. Haus, "Negative refraction and sub-wavelength focusing in the visible range using transparent metallo-dielectric stacks," *Opt. Express*, Vol. 15, 508, 2007.
25. Liu, Y., G. Bartal, and X. Zhang, "All-angle negative refraction and imaging in a bulk medium made of metallic nanowires in the visible region," *Opt. Express*, Vol. 16, 15439, 2008.
26. Song, Z. and W. Jian, "Splitting the surface wave in metal/dielectric nanostructures," *Chinese Phys. B*, Vol. 20, 067901, 2011.

27. Yeshchenko, O., I. Bondarchuk, S. Malynych, Y. Galabura, G. Chumanov, and I. Luzinov, "Surface plasmon modes of sandwich-like metal-dielectric nanostructures," *Plasmonics*, Vol. 10, 655, 2015.
28. Dong, Z., M. Bosman, D. Zhu, X. M. Goh, and J. K. Yang, "Fabrication of suspended metal-dielectric-metal plasmonic nanostructures," *Nanotechnology*, Vol. 25, 135303, 2014.
29. Agranovich, V. M. and V. E. Kravtsov, "Notes on crystal optics of superlattices," *Solid State Commun.*, Vol. 55, 85, 1985.
30. Iorsh, I., A. Orlov, P. Belov, and Y. Kivshar, "Interface modes in nanostructured metal-dielectric metamaterials," *Appl. Phys. Lett.*, Vol. 99, 151914, 2011.
31. Raether, H., *Surface Polaritons*, in V. M. Agranovich, D. L. Mills, (Eds.), *Surface Plasmons*, Springer, New York, 1988.
32. Alu, A., N. Engheta, and R. W. Ziolkowski, "FDTD analysis of the tunneling and growing exponential in a pair of epsilon-negative and mu-negative slabs," *Phys. Rev. E*, Vol. 74, 016604, 2006.
33. Johnson, P. B. and R. W. Christy, "Optical constants of the noble metals," *Phys. Rev. B*, Vol. 6, 4370, 1972.
34. Liu, Z., H. Lee, Y. Xiong, C. Sun, and X. Zhang, "Far-field optical hyperlens magnifying sub-diffraction-limited objects," *Science*, Vol. 315, 1686, 2007.
35. Kim, J., V. P. Drachev, Z. Jacob, G. V. Naik, A. Boltasseva, E. E. Narimanov, and V. M. Shalaev, "Improving the radiative decay rate for dye molecules with hyperbolic metamaterials," *Opt. Express*, Vol. 20, 8100–8116, 2012.
36. Tumkur, T., G. Zhu, P. Black, Yu. A. Barnakov, C. E. Bonner, and M. A. Noginov, "Control of spontaneous emission in a volume of functionalized hyperbolic metamaterial," *Appl. Phys. Lett.*, Vol. 99, 2011. 151115,
37. Tumkur, T. U., L. Gu, J. K. Kitur, E. E. Narimanov, and M. A. Noginov, "Control of absorption with hyperbolic metamaterials," *Appl. Phys. Lett.*, Vol. 100, 161103, 2012.
38. Rho, J., Z. Ye, Y. Xiong, X. Yin, Z. Liu, H. Choi, G. Bartal, and X. Zhang, "Spherical hyperlens for two-dimensional sub-diffractional imaging at visible frequencies," *Nature Commun.*, Vol. 1, 143, 2010.